Force Chains, Microelasticity and Macroelasticity

C. Goldenberg[1,*] and I. Goldhirsch[2,†]

[1]*School of Physics and Astronomy, Tel-Aviv University, Ramat-Aviv, Tel-Aviv 69978, Israel*
[2]*Fluid Mechanics and Heat Transfer, Tel-Aviv University, Ramat-Aviv, Tel-Aviv 69978, Israel*

(Dated: December 28, 2001)

It has been claimed that quasistatic granular materials, as well as nanoscale materials, exhibit departures from elasticity even at small loadings. It is demonstrated, using 2D and 3D models with interparticle harmonic interactions, that such departures are expected at small scales [below $\mathcal{O}(100)$ particle diameters], at which continuum elasticity is invalid, and vanish at large scales. The models exhibit force chains on small scales, and force and stress distributions which agree with experimental findings. Effects of anisotropy, disorder and boundary conditions are discussed as well.

PACS numbers: 45.70.Cc, 46.25.Cc, 83.80.Fg, 61.46.+w

There are at least two classes of systems whose apparent departure from elastic mechanical response, even for infinitesimal loads, has been recently discussed in the literature: granular [1] and nanoscale [2] materials. These two classes share a common property: both are typically composed of a relatively small number of constituents, macroscopic grains in the former and *atoms* in the latter case. Nanoscale grains are not considered here. The discussion below, though relevant to both classes, is worded in "granular terms" and focuses on granular materials.

Models whereby forces in static granular matter "propagate" (corresponding to hyperbolic or parabolic PDE's) have been suggested [3, 4]. This mechanism is in marked contrast with the non-propagating nature of the classical equations of static elasticity (elasto-plastic models are successfully used by engineers in this field [5, 6]).

One of the goals of this Letter is to show that some recent experiments [7, 8], in which the quasi-static response of granular matter has been measured, are consistent with an elastic description, up to differences which stem from the fact that continuum elasticity is a macroscopic theory, valid only above a certain spatial scale. A crossover between microelasticity, i.e., the small scale response of a system whose constituents interact by harmonic forces, and continuum elasticity ('macroelasticity') at large scales is demonstrated. Note that both the response of small (elastic) systems and the short distance response of *any* such system are microelastic.

Any particle in a granular medium experiences interactions with a finite number of other particles, each of which defines a different direction. Therefore the local environment of a particle is not isotropic. The existence of preferred directions on the particle scale implies the possible emergence of force chains, i.e., chains of contacts along which the forces are e.g., stronger than the mean interparticle force. This fact does not preclude elasticity, e.g., the forces may be derived from a potential (and can be linearized) yielding a set of discrete elliptic equations. The notion of force propagation along force chains is merely an *approximation* pertaining to the "strong" forces. Continuum theory cannot be expected to describe these microscopic interparticle *forces*. The macroscopic field which is related to the microscopic forces is the *stress*. Even at small but finite spatial resolution, the stress tensor is determined by an appropriate average over forces, and it may bear little or no resemblance to the force distribution on the microscopic (particle) scale. Though the stress field is well defined on small scales, the constitutive relations correspond to continuum elasticity only on sufficiently large scales. In particular, disorder can have a large effect at small scales, yet allow for large scale homogeneous (and possibly isotropic) elasticity.

The discussion below does not apply to isostatic systems or systems at incipient failure, where particle rearrangements are prominent and the range of validity of elasticity may be extremely limited. We consider only dense systems (which form the majority of granular systems in practical applications) where geometrical constraints and friction prevent major rearrangements for sufficiently small loads (depending on the yield stress).

Consider a two dimensional (2D) collection of uniform disks resting in a finite enclosure (with a horizontal 'floor') under the influence of gravity. A unit downward vertical force is applied at the top of the system (in the simulations below the force acts in the middle of the upper layer). Fig. 1 presents the results of a simulation in which the disks are assumed to interact by uniform linear forces ('springs' whose rest length is the particle diameter). Force chains are evident. Since non-cohesive grains cannot experience tensile forces, we have repeated the simulation with a more realistic interaction in which 'one-sided springs' (which can exert only compressional forces) have been employed. The resulting force distribution is depicted in Fig. 2. Though in the second simulation there is particle rearrangement (some contacts are severed, as observed in [9] for a pile geometry) the appearance of the force chains in both systems is very similar. The force distribution vs. the horizontal coordinate, at different depths, corresponding to Fig. 1, is presented in Fig. 3, and that corresponding to Fig. 2 is presented in Fig. 4. These force distributions are qualitatively similar though the latter (Fig. 4) is far closer to the experimental find-

ings [7] on a similar system of disks (since it better represents the properties of the grains). Furthermore, Fig. 5 presents the force chains for a random network, obtained by adding a random number, uniformly distributed in the range $[-\frac{d}{4}, \frac{d}{4}]$, to the x and y coordinates of points on a triangular lattice with lattice constant, d (except those of the bottom row), with springs connecting points whose distance is less than $c_{\max} = 1.2d$. The results are again qualitatively similar to those obtained in the experiment [7], the main difference with respect to the case of a regular lattice being the fact that here the force chains are somewhat shorter.

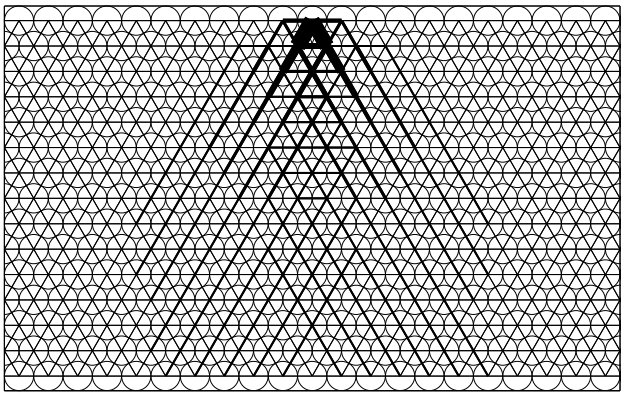

FIG. 1: Force chains in a 2D triangular lattice. A unit vertical force is applied to the center particle in the top layer, with no gravity. Line widths for all the lines shown are proportional to the forces. The central region of the lattice is shown (the entire lattice comprises 15 layers of 41 particles each).

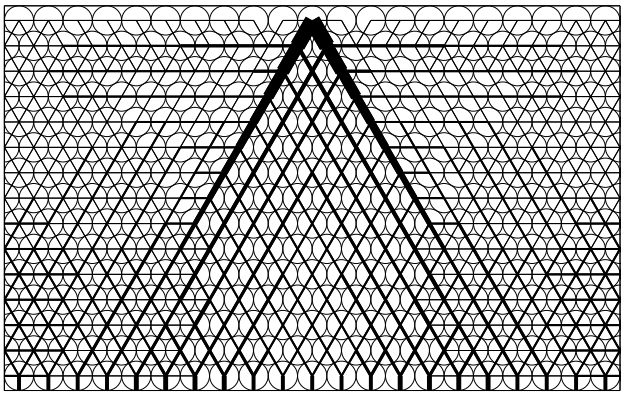

FIG. 2: Force chains in the same 2D triangular lattice as in Fig. 1, but with one-sided springs and gravity.

Fig. 6 depicts the normal vertical stress component, σ_{zz}, corresponding to the system in Fig. 1, as calculated using the following exact formula [10]:

$$\sigma_{\alpha\beta}(\mathbf{r}, t) = \frac{1}{2} \sum_{j \neq i} f_{i/j\alpha}\, r_{ij\beta} \int_0^1 ds \phi(\mathbf{r} - \mathbf{r}_i(t) + s\mathbf{r}_{ij}(t)),$$

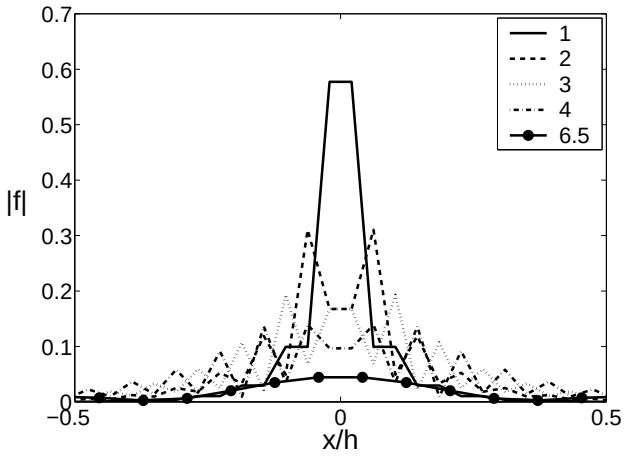

FIG. 3: The norms of the interparticle forces, $|\mathbf{f}|$, in the system depicted in Fig. 1, vs. the horizontal position, x, at several depths. The legend indicates the depth measured from the top, in layer numbers.

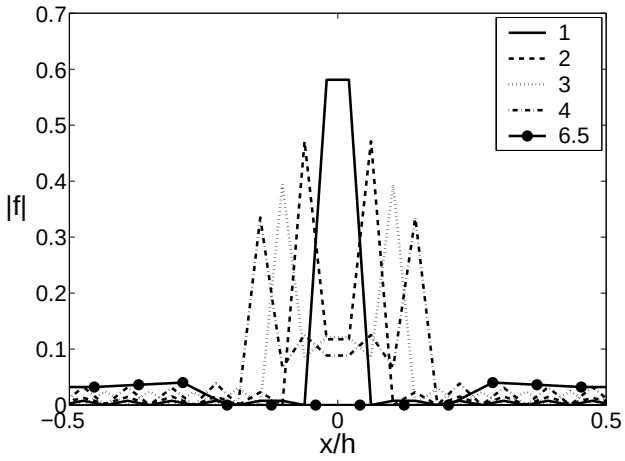

FIG. 4: Same as Fig. 3, for the case of one-sided springs.

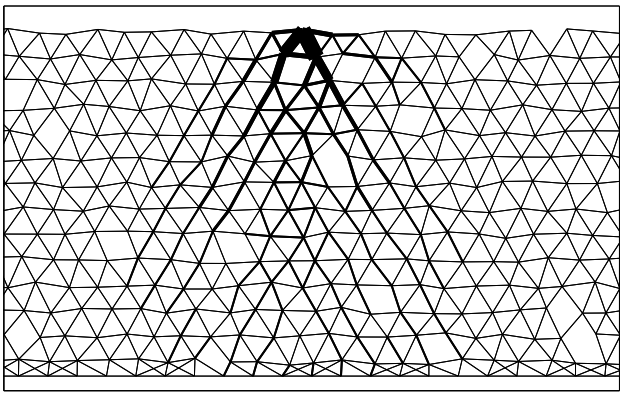

FIG. 5: Force chains in a random network of springs with $c_{\max} = 1.2d$ (see text).

where $\mathbf{r}_i(t)$ is the center of particle i, $\mathbf{r}_{ij}(t) \equiv \mathbf{r}_i(t) - \mathbf{r}_j(t)$,

and $\mathbf{f}_{i/j}$ is the force exerted on particle i by particle j. Greek indices denote Cartesian components. The coarse graining function [10] is $\phi(\mathbf{r}) = \frac{1}{\pi w^2} e^{-(|\mathbf{r}|/w)^2}$, with $w = d$, the particle diameter, i.e., a fine resolution. The force chains are not evident any more. The model considered here corresponds, in the continuum limit, to an isotropic 2D elastic medium [11]. Therefore one can compare the stress obtained from the microscopic force distribution with that of the corresponding elastic solution.

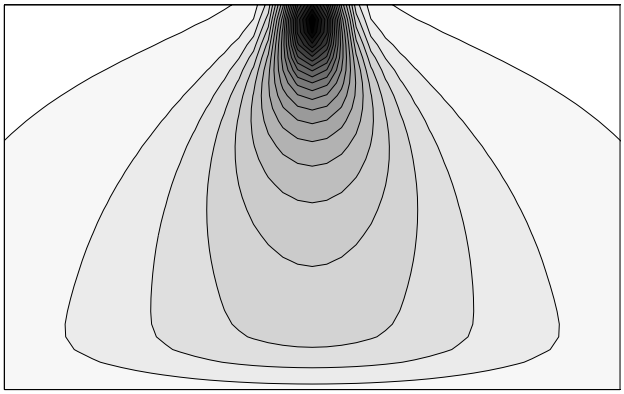

FIG. 6: Contour plot of $h\sigma_{zz}$, in the 2D triangular lattice, in the region shown in Fig. 1. The contour spacing is 0.3. Darker shades indicate larger values of $|\sigma_{zz}|$.

Fig. 7 compares the vertical stress at the floor of the system with elastic solutions for a finite slab (with rough or frictionless support) and a half plane. The convergence to the experimentally appropriate [8] (rough support) solution for a sufficient number of layers is evident. For the random system depicted in Fig. 5, the results are quite similar, expect for (expected) fluctuations.

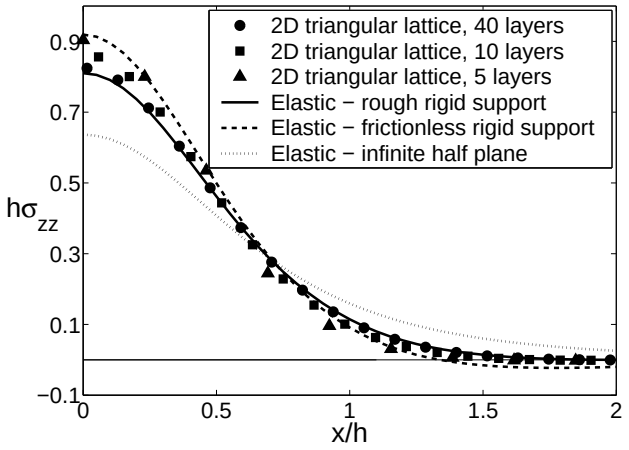

FIG. 7: $h\sigma_{zz}$ at the bottom of the 2D triangular lattice, compared to continuum elastic solutions. The applied force is unity. Note: $\sigma_{zz}\left(\frac{x}{h}\right) = \sigma_{zz}\left(-\frac{x}{h}\right)$.

Consider next an anisotropic medium, obtained by taking the spring constants for contacts in the horizontal direction (parallel to the slab floor), K_1, to be different from those for the contacts in the oblique direction, K_2. As shown in Fig. 8, the obtained stress distribution (on the floor) is either single peaked (narrower than the isotropic one for $K_2/K_1 < 1$, wider for $K_2/K_1 > 1$) or double peaked for sufficiently large K_2/K_1. A similar double peaked distribution is obtained for the case of 'one-sided' springs, where some horizontal contacts are severed, corresponding to the limit $K_2/K_1 \to \infty$ for these contacts. This is evident in Fig. 9, which clearly shows a macroscopic anisotropy (compare to the macroscopically isotropic case shown in Fig. 6). These double peaked distributions are similar to those obtained from hyperbolic models. The results presented here indicate that phenomena similar to those suggested by the hyperbolic models can be obtained using *anisotropic* elasticity. The equations of anisotropic elasticity, which are of course elliptic, can approach hyperbolicity in the limit of very large anisotropy (as mentioned in [3]).

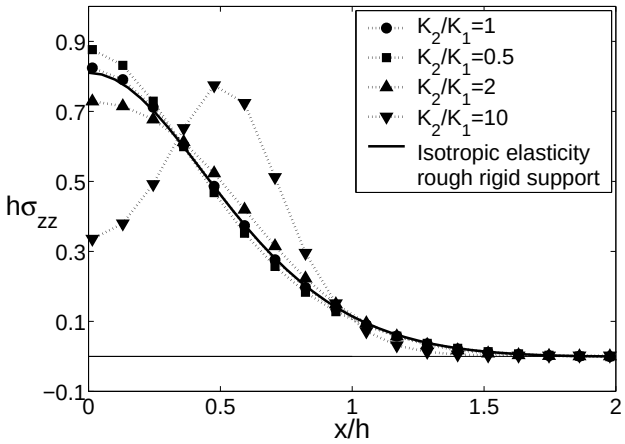

FIG. 8: $h\sigma_{zz}$ at the bottom of anisotropic triangular lattices composed of 40 layers, compared to the isotropic elastic solution. The applied force is unity. Note: $\sigma_{zz}\left(\frac{x}{h}\right) = \sigma_{zz}\left(-\frac{x}{h}\right)$.

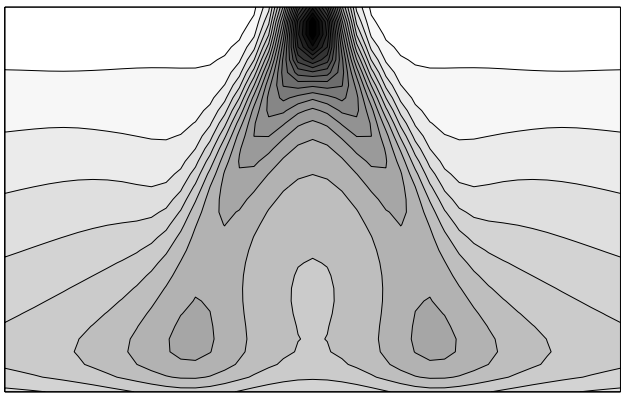

FIG. 9: Same as Fig. 6, for the case of one-sided springs.

Very similar results to those presented above are ob-

tained for a three dimensional (3D) system: consider a collection of particles positioned on a simple cubic lattice. As shown in [12], this system corresponds, on large scales, to an isotropic elastic continuum when the spring constants for springs coupling nearest neighbors equal those coupling next nearest neighbors. While this model clearly does not describe the interaction of granular particles, we believe it is useful for the description of the crossover between microelasticity and macroelasticity. Furthermore, as shown below, the stresses computed for this model are in close correspondence with the experimental results reported in [8]. Consider a 3D slab of finite height, with a downward unit force acting on a particle in the top layer. As in the 2D case described above, the results for discrete lattices converge to the appropriate finite slab elastic solution with increasing depth (Fig. 10). The effect of small scale anisotropy (here, the cubic symmetry) is seen in Fig. 11, which depicts contour plots of the distribution of the vertical stress on the floor. The underlying cubic symmetry is evident for a small depth of the system and is washed out for larger systems, where continuum elasticity holds.

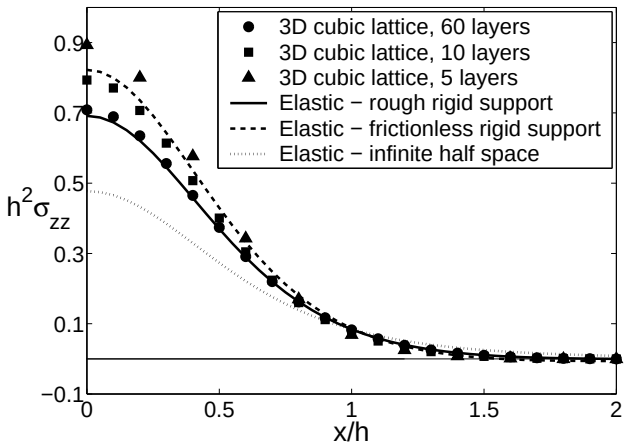

FIG. 10: $h^2\sigma_{zz}$ along the x-axis at the bottom of a cubic lattice, compared to continuum elastic solutions. The results are scaled by h. Note: $h^2\sigma_{zz}\left(\frac{x}{h}\right) = h^2\sigma_{zz}\left(-\frac{x}{h}\right)$.

Our results for a shallow discrete slab are similar to those obtained experimentally for a 'loose' granular packing [8], for which the stress distribution is narrower than that predicted by continuum elasticity. In contrast, for a dense packing, experiments show a wider distribution. As mentioned in [8] and above, this can be explained by anisotropic effects (recall that the above anisotropic 2D system can exhibit both narrower and wider distributions). The method of preparation of the experimental system [8] suggests that a relevant model may consist of a number of isotropic elastic layers of variable moduli. Indeed, in this case the stress distribution on the floor can be wider or narrower than the solution for a homogeneous slab, depending on the distribution of moduli of the layers [6, 11]. In addition, the stress distribution becomes wider the smaller the rigidity of the support [6, 11].

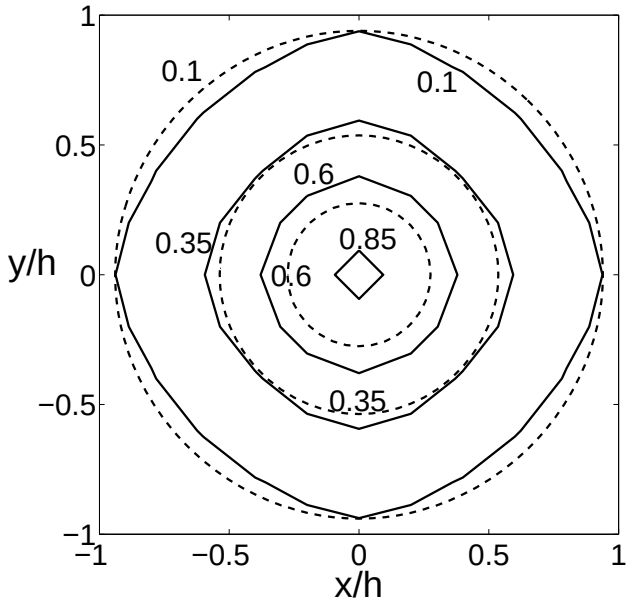

FIG. 11: A contour plot of $h^2\sigma_{zz}$ at the bottom of 3D slabs composed of 5 (solid lines) and 20 (dashed lines) discrete layers. A unit force is applied at the top. The cubic anisotropy is evident for 5 layers, while the distribution appears isotropic for 20 layers.

Support from the Israel Science Foundation, grants no. 39/98 and 53/01, is gratefully acknowledged.

* Electronic address: chayg@post.tau.ac.il
† Electronic address: isaac@eng.tau.ac.il

[1] Focus Issue on Granular Materials, *Chaos* **9** (1999).
[2] e.g., J.-P. Salvetat et al., Appl. Phys. A **69**, 255 (1999); J. Broughton et al., Phys. Rev. B **56**, 611 (1997).
[3] M. E. Cates, J. P. Wittmer, J.-P. Bouchaud and P. Claudin, Chaos **9**, 511 (1999) and refs. therein.
[4] S. N. Coppersmith et al., Phys. Rev. E **53**, 4673 (1996); F. Radjai, S. Roux and J. J. Moreau, Chaos **9**, 544 (1999); J.-P. Bouchaud, P. Claudin, D. Levine and M. Otto, Eur. Phys. J. E **4**, 451 (2001).
[5] R. M. Nedderman, *Statics and Kinematics of Granular Materials* (Cambridge University Press, 1992).
[6] S. B. Savage, in *Powders and Grains 97*, 185, Ed. R. P. Behringer and J. T. Jenkins (Balkema, 1997).
[7] J. Geng et al., Phys. Rev. Lett. **87**, 035506 (2000).
[8] G. Reydellet and E. Clément, Phys. Rev. Lett. **86**, 3308 (2001); D. Serero et al., Eur. Phys. J. E **6**, 169 (2001).
[9] S. Luding, Physical Review E **55**, 4720 (1997).
[10] B. J. Glasser and I. Goldhirsch, Phys. Fluids **13**, 407 (2001).
[11] C. Goldenberg and I. Goldhirsch, unpublished.
[12] C. Kittel, *Introduction to Solid State Physics (Second Edition)* (Wiley, 1956).